Journal of Hazardous Materials 180 (2010) 106–114

Contents lists available at ScienceDirect

Journal of Hazardous Materials

journal homepage: www.elsevier.com/locate/jhazmat

Characterization of pore-expanded amino-functionalized mesoporous silicas directly synthesized with dimethyldecylamine and its application for decolorization of sulphonated azo dyes

Hong Yang[a,b,*], Qiyan Feng[a,b]

[a] School of Environmental Science and Spatial Informatics, China University of Mining and Technology, South 3rd Ring Road, Tongshan District, Xuzhou, Jiangsu 221116, PR China
[b] Jiangsu Key Laboratory of Resources and Environmental Information Engineering, South 3rd Ring Road, Tongshan District, Xuzhou, Jiangsu 221116, PR China

ARTICLE INFO

Article history:
Received 18 November 2009
Received in revised form 1 March 2010
Accepted 27 March 2010
Available online 3 April 2010

Keywords:
Direct synthesis
Expanded pore
Mesoporous silicas
Decolorization
Sulphonated azo dye

ABSTRACT

With dimethyldecylamine (DMDA) as the expander, a new kind of pore-expanded amino-functionalized mesoporous silicas (PEAFMS) was directly synthesized under mild alkali condition. The characteristics of PEAFMS sample demonstrated that the presence of DMDA markedly augmented the average pore diameter (19.04 nm) and strongly enhanced its decolorization ability. Subsequently, acid mordant dark yellow GG (YGG) and reactive red violet X-2R (RVX) were chosen to assess its adsorption capacity for sulphonated azo dyes. The effect of initial pH was investigated and the decolorization mechanism was illuminated. Three isotherms were conducted and the goodness of fit increased as the following order: Freundlich < Langmuir < Redlich–Peterson. The maximum adsorption capacities of YGG and RVX onto PEAFMS were 1.967 and 0.957 mmol/g, respectively. Adsorption kinetic processes were better predicted by the pseudo-second-order rate equation than the pseudo-first-order one. Adsorption thermodynamic results suggested that the adsorption behavior of both dyes onto PEAFMS was spontaneous with the chemical nature. In addition, the regeneration of PEAFMS was proved to be feasible using NaOH as the strippant. After five cycles, PEAFMS still possessed a favorable adsorption capacity for dyes. It is safely concluded that PEAFMS could be a potential adsorbent for the dye removal from wastewater.

1. Introduction

Sulphonated azo dyes, as the most numerous of synthetic azo dyes [1], are extensively used in textile, leather and many other industries. Such dyes easily endanger environment and human for their good water solubility, poor biodegradability and latent mutagenicity/carcinogenicity [2,3]. Therefore, conventional methods of municipal sewage disposal are unfit for dye wastewater. Adsorption is an attractive technology in terms of flexibility, water reuse and waste recovery, simplicity of design, ease of operation and insensitivity to toxic pollutants. The performance of adsorbents is usually the key influence on decolorization. Moreover, the adsorption capacity of adsorbents mainly depends on various characteristics such as surface area, pore structure, loaded functional groups, etc.

Activated carbon is the most popular adsorbent [4,5], but its pores are principally distributed in the micropore (pore size <2 nm) region and restrict its application to only smaller organic molecules (C_3–C_7) [6]. So larger molecules such as dyes cannot easily penetrate into the micropores and efficiently adsorb on them. As a consequence, activated carbon shows the unsatisfactory adsorption capacity for dyes [7–9]. And certain factors such as high cost and regeneration trouble also limit its further applications. In recent years, alternative adsorbents have been investigated, such as castor seed shell [10], rice straw [11], sawdust [12], perlite [13], durian peel [14], coconut-husk [15], kaolinite clay [16], chitosan [17] and soybean hull [18] etc. Most of these alternative adsorbents are easily available and are of low-cost; however, present obvious deficiencies are poor mechanical and heat resistance, relatively high loss ratio and limited adsorption capacity for dyes. So researchers are still impelled to novel adsorbents. And mesoporous silicas modified with various functional groups are attracting more and more attention.

Recently, different kinds of functionalized mesoporous silicas have been reported to be effective adsorbents for dyes and the decolorization efficiency of mesoporous silicas is highly

* Corresponding author at: School of Environmental Science and Spatial Informatics, China University of Mining and Technology, South 3rd Ring Road, Tongshan District, Xuzhou, Jiangsu 221116, PR China. Tel.: +86 516 83882065; fax: +86 516 83591316.
E-mail address: caroline_yanghong@hotmail.com (H. Yang).

0304-3894/$ – see front matter © 2010 Elsevier B.V. All rights reserved.
doi:10.1016/j.jhazmat.2010.03.116

dependent on the pore size [19–22]. Due to larger pore channels and better pore connectivity of pore-expanded mesoporous silicas, specific functional groups modified on the silica surface can interact with various adsorbates more efficiently (e.g. amino groups show excellent adsorption properties for sulphonated azo dyes) [23,24]. Accordingly, there is a great need to expand mesopores for dye removal, although pore expansion easily led to a decrease of ordered mesostructure. In fact, long-range ordering of mesopores and very narrow pore size distributions (PSDs) are not necessary for wastewater treatment [25,26].

Many expanders (e.g. alkanes [27], amines [25] and trimethylbenzene [28]) have been used for pore expansion of mesoporous materials and long-chain amines have revealed the remarkable effect on the enlargement of the pore size. It was reported that the addition of large amounts of dimethyldecylamine (DMDA), favored formation of extra-large mesostructure without functional groups: the pore volume reached up to 3.3 cm^3/g and the pore size was enlarged from 3.5 to 13.5 nm [29]. The presented experimental data showed that characteristics of the resultant mesostructure were closely related to the dosage of DMDA.

At present, most efforts have been focused on two-step synthesis of pore-expanded mesoporous silicas containing functional groups [23,28], that is, the two processes (pore expansion and modification of organic groups) are accomplished individually. Little work has been carried out on direct synthesis of such mesoporous adsorbents. Actually, direct synthesis is more convenient and practical, owing to the incorporation of "pore expansion" and "functionalization" processes in "one-step" procedure. In addition, common solvents and expanders used in the synthesis process, such as trimethylbenzene [28] and xylene [30], are generally harmful to the environment. It is necessary to reduce the toxicity of solvents and expanders even choose harmless ones in view of green chemistry.

In this study, harmless reagents were selected and the direct synthesis of pore-expanded amino-functionalized mesoporous silicas (PEAFMS) was attempted under mild alkali condition for decolorization of sulphonated azo dyes. To illuminate the characterization of PEAFMS and its decolorization ability, amino-functionalized mesoporous silicas without DMDA expanded (AFMS) was also synthesized. The synthetic adsorbents were characterized and their decolorization abilities were subsequently investigated using acid mordant dark yellow GG (YGG) and reactive red violet X-2R (RVX) as model dyes. The effects of initial pH value of dye solutions and adsorption temperature on PEAFMS were studied. Its isothermal, kinetic and thermodynamic adsorption properties were also discussed; moreover, its regeneration performance was evaluated.

2. Materials and methods

2.1. Reagents and materials

3-Aminopropyltriethoxysilane (APTES, 99%) and dimethyldecylamine (DMDA, 97%) were purchased from Aldrich. Tetraethyl orthosilicate (TEOS), cetyltrimethylammonium (CTAB), absolute ethyl alcohol, $NaHCO_3$, HCl, HNO_3 and NaOH were purchased from Shanghai Chemical Co. and tetramethylammonium hydroxide (TMAOH, 25 wt%) was provided by Zhenfeng Chemical Co. Two sulphonated azo dyes, acid mordant dark yellow GG (YGG) and reactive red violet X-2R (RVX), were of commercial grade and obtained from Taopu Dyestuff Co. in Shanghai; their chemical structures, molecular weights and wavelengths corresponding to the maximum adsorbance (λ_{max}) are shown in Table 1. All the above materials were used without further purification. Deionized water was used throughout this work.

2.2. Direct synthesis of PEAFMS and AFMS

The direct synthesis of PEAFMS with DMDA as expander was carried out at room temperature, using APTES, TEOS, TMAOH, CTAB, ethanol and DMDA in relative molar ratios of 1.333:5.333:1.667:1:217.4:1.5. CTAB (2.19 g) was dissolved in 40 g dry ethanol; then, 1.66 g of DMDA was slowly added under vigorous stirring. Meanwhile, 1.76 g of APTES was stirred with 20 g of dry ethanol; subsequently, 3.6 g of 25% TMAOH aqueous solution was dropwise added. Two hours later, the above two solutions were mixed, followed by dropwise adding of TEOS (6.64 g). Then the mixture was slowly stirred for further 1 h. After reaction, the product was transferred into a Petri dish for solvent evaporation at room temperature. The resulting solid was aged in deionized water at 368 K for 2 d. After recovered by filtration, the solid product was refluxed in ethanol/HCl for 1 d at 343 K to extract the surfactant templates. Then it was filtered, stirred in 1 mol/L $NaHCO_3$ solution overnight and washed with deionized water for neutralization. Finally, it was dried under vacuum at 333 K for 1 d to obtain the powder adsorbent. A procedure similar to which described above was followed, except that 1.66 g DMDA was absent.

2.3. Characterization

Fourier transform infrared (FTIR) spectra were obtained from a Spectrum 2000 FTIR spectrometer (Perkin-Elmer) with the usual KBr pellet method to determine the presence of amino groups in mesoporous silicas. The spectral range was chosen from 4000 to 400 cm^{-1}. Contents of carbon, nitrogen, and hydrogen in the sample were measured from a CHNS/O 2400 elemental analyzer (Perkin-Elmer). The nitrogen adsorption tests were performed at 77 K using ASAP 2010 (Micromeritics, USA) to characterize the surface area and pore structure of the samples by Brunauer–Emmett–Teller (BET) method. The transmission electron microscopy (TEM) images were recorded on a JEM-2010 at an acceleration voltage of 120 kV.

2.4. Adsorption test

Stock solutions (10 mmol/L) of two dyes (YGG and RVX) were prepared with deionized water and dye solutions for adsorption tests were diluted at predetermined concentrations. The batch experiments were conducted at different temperatures. The required pH was adjusted by HCl (1 mol/L) or NaOH (1 mol/L), and the pH values were measured by a PH-meter (PHS-3C, China). The mixture of the synthesized adsorbent and the used dye were shaken for 1 h at 150 rpm. Then the resulting mixture was filtered through a 0.45 μm Uniflo filter unit and the filtrate was analyzed via a UV–vis spectrophotometer (UV-160A, Shimadzu, Japan) after appropriate dilution.

2.4.1. Comparison of adsorption capacities of two synthesized adsorbents

In a typical run, 100 mg of PEAFMS or AFMS was immersed in 100 mL of dye solution (initial pH 2) at room temperature with variable dye concentrations of 0.3, 0.5, 1.0, 1.5 and 2.0 mmol/L.

In all experiments, the equilibrium adsorption capacity of a given dye onto the adsorbent can be calculated by the change in concentration between the filtrate and the initial dye solution (Eq. (1)):

$$q_e = (C_0 - C_e) \times \frac{V}{W} = \frac{C_0 - C_e}{m} \quad (1)$$

where q_e is the equilibrium adsorption capacity (mmol/g); V is the volume of the aqueous solution (L); W is the dosage of the adsorbent (g); m is the mass concentration of the adsorbent (g/L); C_0 (mmol/L)

Table 1
Chemical structures, molecular weights and λ_{max} of two sulphonated azo dyes.

Dye	Chemical structure	Molecular weight	λ_{max}
YGG	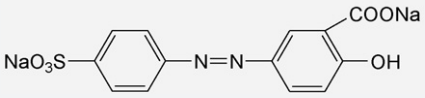	366	356
RVX	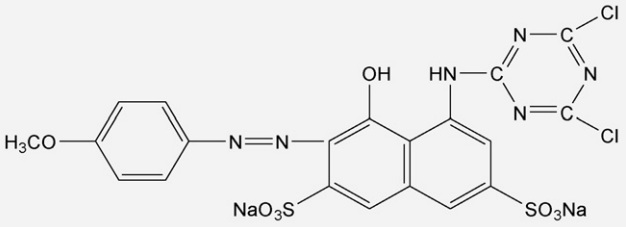	645	532

and C_e (mmol/L) are the initial and equilibrium concentrations of the given dye in the solution, respectively.

2.4.2. Measurement of zeta potential and effect of initial pH

In a typical procedure, 0.005 g of the PEAFMS sample was added to 100 mL of KNO_3 solution (0.1 mol/L) and the pH value of generated suspension was adjusted from 1 to 10 using HNO_3 (0.1 mol/L) or NaOH (0.1 mol/L). After being ultrasonicated for 20 min, 2–4 mL of the suspension was transferred into a measuring cell. The zeta potential was measured at room temperature using a zeta analyzer (Malvern ZS Nano S, Malvern Instrument Inc., London, UK). The procedure was repeated eight times to calculate the mean values of experimental data.

One hundred milligrams of the PEAFMS sample and 100 mL of 0.3 mmol/L YGG solution (pH 1, 2, 3, 4, 5 and 6) were shaken. The adsorption capacity of dyes on adsorbents was measured as a function of initial pH to determine the optimal pH.

2.4.3. Adsorption isotherm test

In a typical run, 100 mg of PEAFMS was immersed in 100 mL of dye solution (pH 2) with variable concentrations of 0.3, 0.5, 1.0, 1.5 and 2.0; then the mixture was shaken at 298 K. The same procedures were followed at 288 and 308 K, respectively.

2.4.4. Adsorption kinetics test

In a typical run, 100 mg of PEAFMS and 100 mL of 2.0 mmol/L YGG solutions (1.0 mmol/L RVX solution) were shaken at 298 K. The same procedures were followed at 288 and 308 K, respectively. The initial pH value of all dye solutions was adjusted at 2.

2.5. Regeneration test of PEAFMS

The YGG-loaded sample was used to verify the regeneration performance of PEAFMS. In a typical run, 100 mg of PEAFMS and 100 mL of 1.0 mmol/L YGG solution (pH 2) were shaken at 298 K. Then the dye-loaded adsorbent was placed in 200 mL of 0.5 mol/L NaOH, stirred for 4 h to elute dye molecules at 323 K. After filtration, the adsorbent was washed and neutralized with ethanol and deionized water. Following another filtration, the adsorbent was dried in a vacuum oven at 333 K before the next cycle. Five sequential cycles of adsorption–desorption were carried out.

3. Results and discussion

3.1. Characterization of the synthetic PEAFMS and AFMS

The synthesized adsorbents were ground and sieved. And the particle size ranged from 120 to 170 BSS mesh size. As Sayari and co-workers reported [29], the dosage of expander (DMDA) has a primary effect on the resultant mesostructure. Based on preliminary tests, DMDA/CTAB molar ratio of 1.5 was screened for the synthesis of PEAFMS. Fig. 1 displays the FTIR spectrum of PEAFMS and AFMS samples. It is confirmed that not only the absence of DMDA but also its presence can realize the successful incorporation of $-NH_2$ in the silicate framework. Take PEAFMS as an example, the band at 1634 cm^{-1} is the H_2O vibration; the peaks at 1078, 799 and 465 cm^{-1} indicate Si–O–Si asymmetric stretching vibration, symmetric stretching vibration and bending vibration, respectively; the bands at 2937 and 683 cm^{-1} are attributed to methane asymmetric stretching vibration and rocking vibration, respectively; the characteristic peaks at 1550, 1590 and 3435 cm^{-1} for $-NH_2$ are also the strong evidence for successful grafting of functional groups [31–34]. In comparison with the characteristic peaks of PEAFMS, the slight frequency difference of AFMS possibly results from the change of the infrared activity with the modification of $-NH_2$ [35].

Elemental analysis demonstrated that the modified $-NH_2$ of PEAFMS and AFMS reached a molar content of 2.143 and 2.582 mmol/g, respectively. So another evidence was provided that amino-functionalized mesoporous silicas could be directly prepared with DMDA as the expander. The decrease in the loading of $-NH_2$ mainly resulted from the use of DMDA. DMDA was located not only in the center of surfactant (CTA^+) micelles for pore expansion, but also at the silica–micelle interface [29]. Therefore, the co-condensation of silicates, surrounding the surfactant micelles, was partially weakened by DMDA.

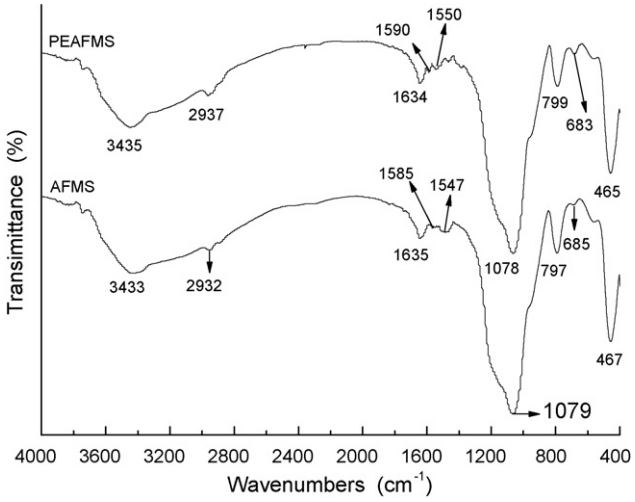

Fig. 1. The FTIR spectrum of the synthetic PEAFMS and AFMS samples.

The nitrogen adsorption tests were performed to observe the mesostructures of the PEAFMS and AFMS samples. Fig. 2a and b exhibit their nitrogen adsorption–desorption isotherms and PSDs, respectively. The isotherms are in accordance with the type-IV curve, which is the characteristic of mesostructures [36]; moreover, the adsorption–desorption hysteresis loop of PEAFMS shifts to a higher relative pressure compared with that of AFMS and reported mesoporous materials swelled by some other expanders [37,38]. This implies that the mesopore size was markedly expanded with DMDA. The mesopore expansion can be further appeared from their PSDs in Fig. 2b. The broader peak on the PSDs of PEAFMS manifested the occurrence of larger mesopores but less uniform mesostructure. The BET surface area, pore volume and pore size of PEAFMS (AFMS) were calculated to be 285.6 (516.3) m^2/g, 1.360 (0.6046) cm^3/g and 19.04 (4.684) nm, respectively. The possible reason of relatively low BET surface area of PEAFMS is partial structural collapse because of the extreme pore size enlargement [25].

The TEM images (Fig. 2c) of two samples correspond to the porosity data determined by the nitrogen adsorption test. The disordered mesostructure of PEAFMS is clearly exhibited due to the use of DMDA. The above characteristic results verify that DMDA is an effective expander and PEAFMS can be directly synthesized with harmless reagents.

3.2. Comparison of adsorption capacities of two synthesized adsorbents

Two important characteristics of an adsorbent, grafted functional groups and pore structures (e.g. pore size and pore volume), have a remarkable influence on the adsorption capacity for given adsorbates. For synthesized adsorbents in this study, the equilibrium adsorption capacity (q_e) was chosen as the evaluating parameter to compare their adsorption capacities for dyes and reflect the effect of DMDA on decolorization.

Fig. 3 presents equilibrium adsorption capacities of YGG and RVX on PEAFMS and AFMS samples, respectively. As a result of different mole numbers of sulphonated groups in the two dye molecules, the adsorption capacity of YGG is about one time higher than that of RVX. The q_e values of two dyes on two adsorbents at all concentrations reveal that PEAFMS has much better decolorization ability than AFMS. The larger pore size of PEAFMS is more favorable to the dye removal, which is similar to the results of some published investigations [20,39]. The dye removal is essentially a surface phenomenon and an interaction between active sites of adsorbents and dye molecules. The adsorption capacity for dyes is strongly impaired owing to the steric clogging, which concerns two or more consecutive active sites may be occupied because of the relatively small pores of AFMS. So properly increasing the pore

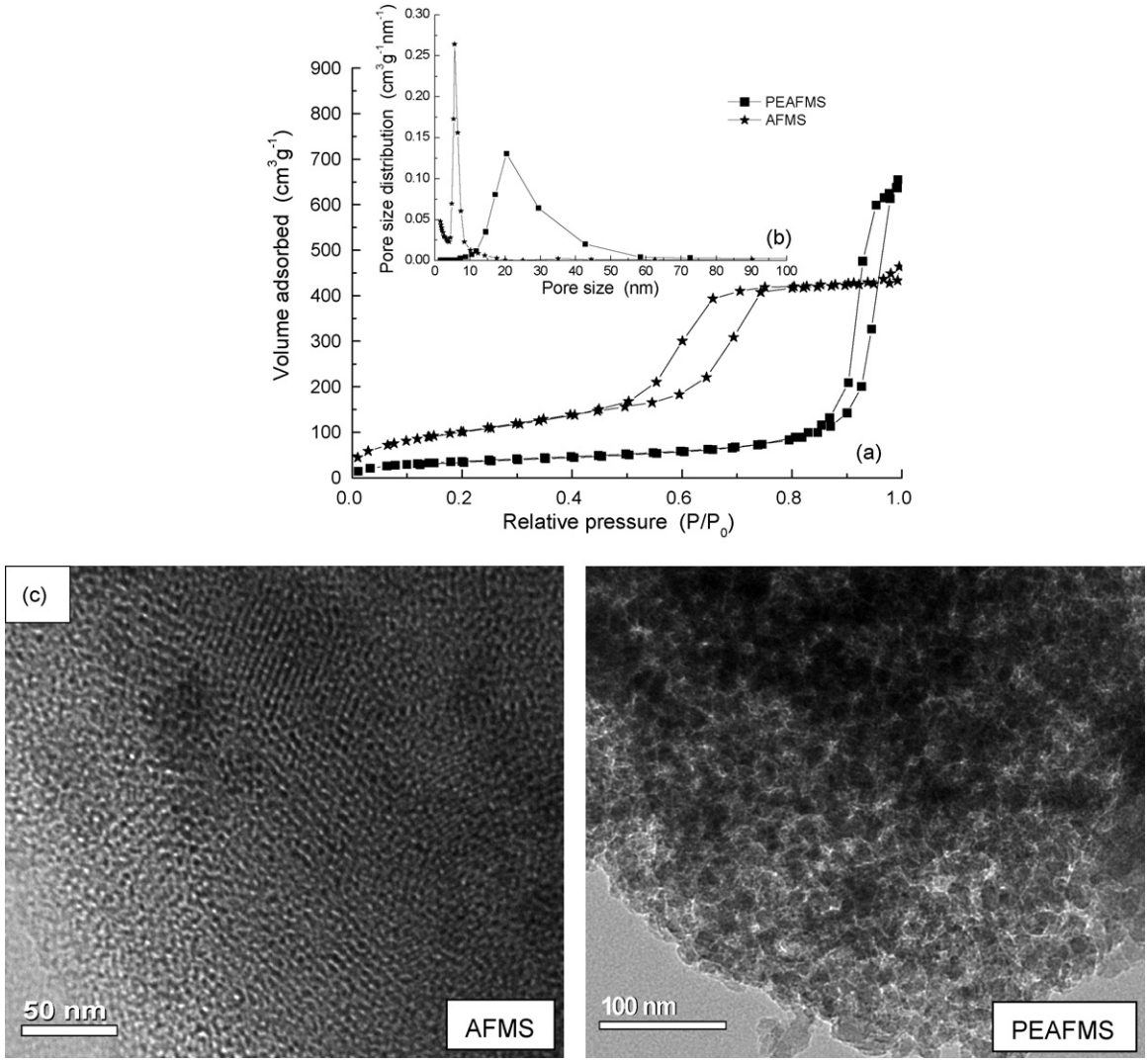

Fig. 2. The nitrogen adsorption–desorption isotherms (a), pore size distribution curves (b) and the TEM images of (c) the synthetic PEAFMS and AFMS samples.

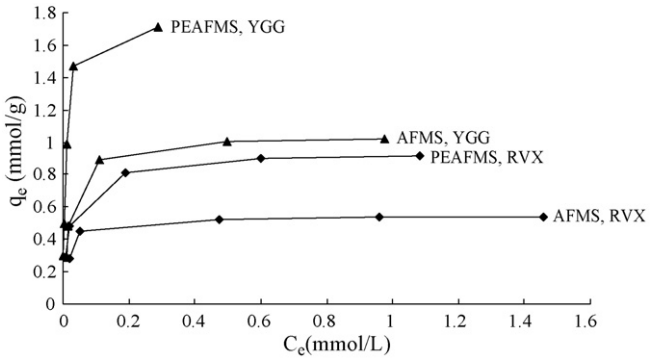

Fig. 3. Equilibrium adsorption capacities of YGG and RVX onto PEAFMS and AFMS samples (solution volume 100 mL and initial pH 2).

size of adsorbents is propitious for reducing the steric clogging and thus enhances their decolorization ability. It is confirmed by experimental data that the appropriate addition of DMDA can greatly improve the porous structures and decolorization performance of mesoporous adsorbents. Thereinafter the decolorization behavior of PEAFMS was investigated.

3.3. Effect of initial pH

The initial pH of dye solutions plays an important role in the protonation of amines and ionization of sulphonated dye molecules. It is essential to investigate the point of zero change (PZC) and the optimal pH value for decolorization. The relation between zeta potential and solution pH is given in Fig. 4a and pH_{PZC} of PEAFMS is estimated to be 6.7. At $pH < pH_{PZC}$, the surface of PEAFMS is positively charged (favor the adsorption of anions) while at $pH > pH_{PZC}$ negatively (favor the adsorption of cations). For the adsorption of sulphonated dyes onto PEAFMS, at $pH < pH_{PZC}$, protonated amines generate positive charge ($R–NH_3^+$); simultaneously, dissociated sulphonic groups load negative charge ($D–SO_3^-$). The consequential decolorization of sulphonated azo dyes can be illuminated according to Eq. (2) [40]:

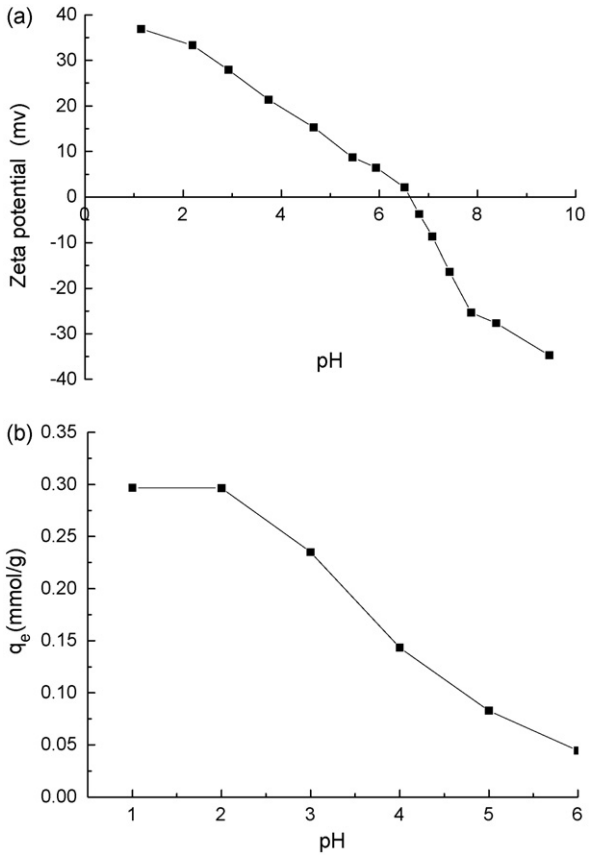

Fig. 4. (a) The relation between zeta potential of PEAFMS and solution pH. (b) Effect of initial pH on the adsorption of YGG onto PEAFMS (T = 298 K, C_0 = 0.3 mmol/L, m = 1 g/L, t = 1 h).

$$R–NH_3^+ + D–SO_3^- \rightarrow R–NH_3^{+\bullet -}O_3S–D \quad (2)$$

YGG was selected as the representative dye to demonstrate the effect of initial pH on the decolorization behavior (Fig. 4b). And the q_e values were calculated according to Eq. (1). Due to $pH_{PZC} < 7$, comparative tests were performed at six pH values: 1, 2, 3, 4, 5 and 6. Fig. 4b displays that decolorization of sulphonated azo dyes was gradually enhanced as pH values decreased, which is consistent with the change of zeta potential in Fig. 4a. With the decrease of pH values, chemical bondings were strengthened and the equilibrium adsorption capacity of YGG onto PEAFMS increased due to the stronger protonation of amines. However, amines were fully protonated so that its decolorization ability could not be further improved when $pH \leq 2$. In addition, adsorption amount of YGG onto PEAFMS dropped sharply at higher pH (>4), which mainly resulted from the combined action of Van der Waals force and hydrogen binding [41,42]. Obviously, the optimal pH value was 2.

3.4. Adsorption isotherms

Langmuir, Freundlich and Redlich–Peterson equations are three common isotherm models to describe the behavior of adsorbents and the correlation between adsorption parameters. In this work, the three models were used to test the adsorption process of PEAFMS.

The basic assumption of Langmuir model [43,44] is that the adsorption takes place at specific homogeneous sites within the adsorbent. Theoretically, maximum adsorption corresponds to a saturated monolayer of adsorbate molecules on the adsorbent surface. The Langmuir isotherm is given as Eq. (3):

$$q_e = \frac{bQ_{max}C_e}{1 + bC_e} \quad (3)$$

where q_e (mmol/g) is the equilibrium loading capacity of adsorbent; C_e and C_0 (mmol/L) are the equilibrium and initial concentration of the adsorbate; Q_{max} (mmol/g) is the maximum adsorption capacity corresponding to complete monolayer coverage; b (L/mmol) is the Langmuir adsorption equilibrium constant.

A dimensionless constant separation factor (R_L) of Langmuir isotherm, is used to determine the favorability of the adsorption process. R_L is defined as Eq. (4). The values of R_L indicate the type of isotherm to be irreversible ($R_L = 0$), favorable ($0 < R_L < 1$), linear ($R_L = 1$) or unfavorable ($R_L > 1$).

$$R_L = \frac{1}{1 + bC_0} \quad (4)$$

The Freundlich isotherm [45,46] is an empirical isotherm and often used for nonideal adsorption that involves heterogeneous surface energy systems. It is expressed by Eq. (5):

$$q_e = K_F C_e^{1/n} \quad (5)$$

where K_F is the Freundlich constant; $1/n$ is the Freundlich exponent. Generally, the adsorption capacity of an adsorbent for a given adsorbate augments with the increase in K_F; the values of $1/n$ imply the adsorption intensity and the type of isotherm to be favorable ($0.1 < 1/n < 0.5$) or unfavorable ($1/n > 2$).

The Redlich–Peterson [47] isotherm combines elements from both the Langmuir and Freundlich models. It can be applied either

Table 2
Langmuir, Freundlich and Redlich–Peterson isotherm parameters and correlation coefficients for removal of YGG and RVX by PEAFMS at 288, 298 and 308 K (m = 1 g/L, t = 1 h, initial pH 2).

Isotherm parameters	YGG			RVX		
	288 K	298 K	308 K	288 K	298 K	308 K
Langmuir model						
b	67.44	135.3	106.9	85.46	127.7	131.7
Q (mmol/g)	1.837	1.967	1.912	0.8368	0.9019	0.9574
R_L	0.007360	0.003683	0.004657	0.005816	0.003900	0.003781
R^2	0.9988	0.9807	0.9949	0.9832	0.9882	0.9744
Freundlich model						
K_F	2.725	3.364	3.063	0.8830	0.9708	1.026
$1/n$	0.2846	0.2783	0.2752	0.1671	0.1636	0.1582
R^2	0.8925	0.8444	0.8722	0.9411	0.9378	0.8896
Redlich–Peterson model						
K	125.3	266.5	205.2	103.6	153.5	129.0
α	67.79	135.3	107.0	120.4	164.8	134.2
β	0.9958	0.9993	0.9985	0.9361	0.9450	0.9939
R^2	0.9988	0.9807	0.9949	0.9982	0.9998	0.9746

in homogenous or heterogeneous systems. This model can be represented as following:

$$q_e = \frac{KC_e}{1 + \alpha C_e^{\beta}} \tag{6}$$

where K and α are the Redlich–Peterson constants; β is the exponent which has a value between 0 and 1. For high concentrations, Eq. (6) reduces to the Freundlich isotherm (Eq. (5)); for β = 1, Eq. (6) reduces to the Langmuir isotherm (Eq. (3)).

The experimental data for the equilibrium adsorption of both dyes on PEAFMS have been fitted to the Langmuir, Freundlich and Redlich–Peterson isotherms. The calculated isotherm constants and correlation coefficients are listed in Table 2. It is clear that PEAFMS has the obviously greater decolorization performance than some reported counterparts [19–22] for the pore expansion of DMDA. As a result of different mole numbers of sulphonated groups in the two dye molecules, the adsorption capacity of YGG is about one time higher than that of RVX.

As shown in Table 2, the values of R_L and $1/n$ all indicate that PEAFMS is a favorable adsorbent for removal of sulphonated azo dyes from effluents. Simultaneously, the R^2 values of three isotherm models increase as the following order: Freundlich < Langmuir < Redlich–Peterson. The best fit of Redlich–Peterson model is reasonable due to its incorporation of Langmuir and Freundlich models. And the higher R^2 values of Langmuir model demonstrate that the adsorption behavior of PEAFMS for the above dyes (especially for YGG) mostly belonged to monolayer adsorption.

The presented values of Q_{max} in Table 2 illuminate that most grafted amines of PEAFMS reacted with sulphonic groups of dyes; the maximum adsorption capacities of YGG and RVX onto PEAFMS have reached 1.967 mmol/g (298 K) and 0.957 mmol/g (308 K), respectively. This is full proof that enlarged pores of PEAFMS can enhance the diffusion of dye molecules across the external and in the internal surface of adsorbent particles [21]. Therefore, the pore expansion by DMDA undoubtedly redounds to the adsorption capacity of given dyes. Furthermore, in the range of test temperature (from 288 to 308 K), Q_{max} values of YGG and RVX have different trends with increasing temperature: for RVX, the adsorption amount always increased; however, for YGG, the adsorption amount increased and then decreased. The possible reason is that the acceleration in the rates of adsorption and desorption vary with temperature rise for the complexity of dye molecules [48,49]. Generally, simple dye molecules (e.g. YGG) are desorbed easier than complex ones (e.g. RVX); thus the adsorption amount of YGG earlier decreased than that of RVX.

3.5. Adsorption kinetics

The adsorption rate is an important parameter used to image the adsorption process. Many applications, such as wastewater treatment and dye removal, need rapid adsorption rate and short contact time.

The pseudo-first-order and pseudo-second-order kinetic models are commonly used to estimate the rate constants, initial adsorption rates and adsorption capacities of an adsorbent for some adsorbates. Two nonlinear models can be expressed as Eqs. (7) and (8) [50–52]:

$$q_t = q_e(1 - \exp^{-k_1 t}) \tag{7}$$

$$q_t = \frac{k_2 q_e^2 t}{1 + k_2 q_e t} \tag{8}$$

where t is the contact time (min); q_t (mmol/g) and q_e (mmol/g) are the amount of adsorbate adsorbed at equilibrium and time t, respectively; k_1 (min^{-1}) and k_2 (g/mmol min) are the rate constants of pseudo-first-order and pseudo-second-order adsorption, respectively.

Results of experimental q_e ($q_{e,exp}$), calculated q_e ($q_{e,cal}$) and other parameters are shown in Table 3. The kinetic processes of dye adsorption onto PEAFMS sample are illustrated at 288, 298 and 308 K. Despite slight difference between $q_{e,exp}$ and $q_{e,cal}$ values, the calculated data explain the excellent adsorption attribution of PEAFMS sample again. By contrasting R^2 values, it is found that the pseudo-second-order kinetic model fitted better with kinetic data of PEAFMS than pseudo-first-order kinetic model. This demonstrates that the adsorption behavior over the whole range agrees with the chemisorption mechanism [15].

3.6. Adsorption thermodynamics

The relation between the equilibrium constant (K_0) and Gibbs free energy change (ΔG^0, kJ/mol) of the adsorption process can be obtained from Eq. (9) [52]:

$$\Delta G^0 = -RT \ \ln K_0 \tag{9}$$

where R is the universal gas constant (8.314 J/mol K) and T is the absolute temperature (K). Values of K_0 can be calculated according to Eq. (10) at different temperatures [53]:

$$K_0 = \frac{q_e}{C_e} \tag{10}$$

where q_e (mmol/g) and C_e (mmol/L) are the equilibrium amount of dyes adsorbed on the adsorbent and equilibrium concentration of dyes in the solution, respectively.

Table 3
Pseudo-first-order and pseudo-second-order kinetic parameters for removal of YGG and RVX by PEAFMS at 288, 298 and 308 K (m = 1 g/L, t = 1 h, initial pH 2).

Kinetic parameters	YGG (C_0 = 2 mmol/L)			RVX (C_0 = 1 mmol/L)		
	288 K	298 K	308 K	288 K	298 K	308 K
$q_{e,exp}$ (mmol/g)	1.634	1.727	1.692	0.7767	0.8237	0.8504
Pseudo-first-order model						
$q_{e,cal}$ (mmol/g)	1.600	1.694	1.662	0.7529	0.8024	0.8315
k_1	0.1242	0.1363	0.1348	0.1122	0.1252	0.1450
R^2	0.9879	0.9884	0.9904	0.9850	0.9853	0.9898
Pseudo-second-order model						
$q_{e,cal}$ (mmol/g)	1.706	1.798	1.768	0.8078	0.8566	0.8811
k_2	0.1232	0.1323	0.1298	0.2269	0.2451	0.2891
R^2	0.9980	0.9980	0.9972	0.9987	0.9990	0.9977

Table 4
Thermodynamic parameters for removal of YGG and RVX by PEAFMS.

Dye	ΔH^0 (kJ/mol)	ΔS^0 (J/mol K)	ΔG^0 (kJ/mol)		
			288 K	298 K	308 K
YGG	24.87	98.79	−3.582	−4.570	–
	−10.77	−20.80	–		−4.364
RVX	18.15	73.48	−3.012	−3.747	−4.482

The enthalpy change (ΔH^0, kJ/mol) and entropy change (ΔS^0, J/mol K) for adsorption are related to ΔG^0 by Eq. (11) [52]:

$$\Delta G^0 = \Delta H^0 - T\Delta S^0 \quad (11)$$

The estimated adsorption thermodynamic parameters are presented in Table 4. The negative values of ΔG^0 indicate that the adsorption of two dyes on PEAFMS was spontaneous with the chemical nature in the range of test temperature; however, the values of ΔH^0 and ΔS^0 confirm the different adsorption feature of given dyes. For RVX, the positive value of ΔH^0 illuminates the endothermic adsorption, so raising temperature leads to a higher adsorption capacity; the positive value of ΔS^0 shows the increased disorder at solid–solution interface, so the enhanced entropy motivates the replacement of hydrated dye molecules for water molecules around PEAFMS particles [15,21]. For YGG, the change of ΔH^0 and ΔS^0 (288–298 K) is identical to that of RVX. From 298 to 308 K, the negative value of ΔH^0 reveals the exothermic adsorption and results in the slight decrease of adsorption capacity with increased temperature; although the negative value of ΔS^0 presents the decreased randomness, the spontaneous adsorption process is still formed because the enthalpy contribution is much larger than that of the entropy [15,21].

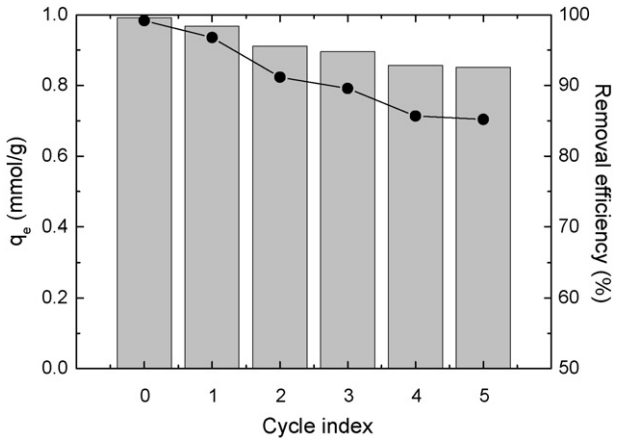

Fig. 5. Adsorption–desorption cycles of the YGG-loaded PEAFMS.

3.7. Regeneration test of PEAFMS

To evaluate the regeneration performance of PEAFMS, sequential adsorption–desorption tests were conducted over five cycles. According to the decolorization mechanism of PEAFMS, it is reasonable that the dye-loaded sample could be recovered under reverse basic condition. Fig. 5 shows the values of q_e and removal efficiencies in every cycle. The regeneration of PEAFMS was proved to be feasible using NaOH as the strippant. The adsorbent removed over 85% of YGG from solutions after five stripping cycles. After five cycles, the nitrogen content of regenerated PEAFMS was determined by elemental analysis. The modification of $-NH_2$ still retained 2.127 mmol/g and the tiny reduction of amino groups (0.016 mmol/g) fully indicated the good stability of its mesostructure. In the first cycle, the PEAFMS sample presented high removal efficiency; however, the reduced adsorption capacity could be attributed to the loss of the adsorbent during each cycle (about 5–8% per cycle). The data demonstrate the relatively excellent regeneration performance of PEAFMS compared to some reported adsorbents [17,50,54].

4. Conclusions

The present work demonstrates that it is possible to use DMDA as the expander to directly synthesize pore-expanded amino-functionalized mesoporous silicas (PEAFMS) with harmless reagents. The DMDA dosage (n_{DMDA}:n_{CTAB} = 1.5) markedly expanded the mesopore size (19.04 nm), and imparted a considerable decolorization ability to the synthesized sample in consequence. The adsorption of two sulphonated azo dyes, YGG and RVX, from aqueous solution onto PEAFMS was studied. Compared to AFMS, PEAFMS has much better adsorption capacity for dyes. The decolorization behavior of PEAFMS was subsequently investigated. Removal of sulphonated dyes was pH dependant and the satisfactory decolorization was attained at initial pH 2. The analysis of R^2 values for adsorption isotherm models showed that the goodness of fit increased as the following order: Freundlich < Langmuir < Redlich–Peterson; and the maximum adsorption capacities of YGG and RVX onto PEAFMS were 1.967 and 0.957 mmol/g, respectively. Adsorption kinetic data exhibited the relatively short equilibrium time (1 h) and the adsorption processes could well be described by the pseudo-second-order

rate equation. Adsorption thermodynamic results suggested that the adsorption behavior of two dyes onto PEAFMS was spontaneous with the chemical nature. The adsorption–desorption tests indicated that the regeneration of PEAFMS was feasible using NaOH as the strippant. After five cycles, PEAFMS still possessed a favorable adsorption capacity of dyes. On the basis of observed experimental data, it is safely concluded that PEAFMS could be a potential adsorbent for the dye removal from wastewater.

Acknowledgments

This research was funded by the National Special Science and Technology Project of China (No. 2009ZX05039-003), the Science Foundation of CUMT (China University of Mining and Technology) for Young Teachers (No. 2008A033) and China Postdoctoral Science Foundation (No. 20090461158). The technical support from Jiangsu Key Laboratory of Resources and Environmental Information Engineering was also appreciated.

References

[1] T. Joshi, L. Iyengar, K. Singh, S. Garg, Isolation, identification and application of novel bacterial consortium TJ-1 for the decolourization of structurally different azo dyes, Bioresour. Technol. 99 (15) (2008) 7115–7121.
[2] G.D.A. Umbuzeiro, H.S. Freeman, S.H. Warren, D.P.D. Oliveira, Y. Terao, T. Watanabe, L.D. Claxton, The contribution of azo dyes to the mutagenic activity of the Cristais River, Chemosphere 60 (1) (2005) 55–64.
[3] A. Pandey, P. Singh, L. Iyengar, Bacterial decolorization and degradation of azo dyes, Int. Biodeterior. Biodegrad. 59 (2) (2007) 73–84.
[4] O. Abdelwahab, Evaluation of the use of loofa activated carbons as potential adsorbents for aqueous solutions containing dye, Desalination 222 (1–3) (2008) 357–367.
[5] J. Yener, T. Kopac, G. Dogu, T. Dogu, Dynamic analysis of sorption of Methylene Blue dye on granular and powdered activated carbon, Chem. Eng. J. 144 (3) (2008) 400–406.
[6] P.B. Venuto, Organic catalysis over zeolites: a perspective on reaction paths within micropores, Microporous Mater. 2 (1994) 297–411.
[7] H. Tamai, T. Kakii, Y. Hirota, T. Kumamoto, H. Yasuda, Synthesis of extremely large mesoporous activated carbons and its unique adsorption for giant molecules, Chem. Mater. 8 (2) (1996) 454–462.
[8] G. Crini, Non-conventional low-cost adsorbents for dye removal: a review, Bioresour. Technol. 97 (9) (2006) 1061–1085.
[9] C. Pelekani, V.L. Snoeyink, Competitive adsorption in natural water: role of activated carbon pore size, Water Res. 33 (5) (1999) 1209–1219.
[10] N.A. Oladoja, C.O. Aboluwoye, Y.B. Oladimeji, A.O. Ashogbon, I.O. Otemuyiwa, Studies on castor seed shell as a sorbent in basic dye contaminated wastewater remediation, Desalination 227 (1–3) (2008) 190–203.
[11] R. Gong, K. Zhong, Y. Hu, J. Chen, G. Zhu, Thermochemical esterifying citric acid onto lignocellulose for enhancing methylene blue sorption capacity of rice straw, J. Environ. Manage. 88 (4) (2008) 875–880.
[12] R. Gong, M. Feng, J. Zhao, W. Cai, L. Liu, Functionalization of sawdust with monosodium glutamate for enhancing its malachite green removal capacity, Bioresour. Technol. 100 (2) (2009) 975–978.
[13] M. Roulia, A.A. Vassiliadis, Sorption characterization of a cationic dye retained by clays and perlite, Microporous Mesoporous Mater. 116 (1–3) (2008) 732–740.
[14] B.H. Hameed, H. Hakimi, Utilization of durian (Durio zibethinus Murray) peel as low cost sorbent for the removal of acid dye from aqueous solutions, Biochem. Eng. J. 39 (2) (2008) 338–343.
[15] R. Jain, M. Shrivastava, Adsorptive studies of hazardous dye Tropaeoline 000 from an aqueous phase on to coconut-husk, J. Hazard. Mater. 158 (2–3) (2008) 549–556.
[16] E.I. Unuabonah, K.O. Adebowale, F.A. Dawodu, Equilibrium, kinetic and sorber design studies on the adsorption of Aniline blue dye by sodium tetraborate-modified Kaolinite clay adsorbent, J. Hazard. Mater. 157 (2–3) (2008) 397–409.
[17] G.Z. Kyzas, N.K. Lazaridis, Reactive and basic dyes removal by sorption onto chitosan derivatives, J. Colloid Interface Sci. 331 (1) (2009) 32–39.
[18] R. Gong, J. Sun, D. Zhang, K. Zhong, G. Zhu, Kinetics and thermodynamics of basic dye sorption on phosphoric acid esterifying soybean hull with solid phase preparation technique, Bioresour. Technol. 99 (10) (2008) 4510–4514.
[19] Z. Wu, H. Joo, K. Lee, Kinetics and thermodynamics of the organic dye adsorption on the mesoporous hybrid xerogel, Chem. Eng. J. 112 (1–3) (2005) 227–236.
[20] S. Wang, H. Li, Structure directed reversible adsorption of organic dye on mesoporous silica in aqueous solution, Microporous Mesoporous Mater. 97 (1–3) (2006) 21–26.
[21] P.V. Messina, P.C. Schulz, Adsorption of reactive dyes on titania–silica mesoporous materials, J. Colloid Interface Sci. 299 (1) (2006) 305–320.
[22] X. Yuan, S.P. Zhuo, W. Xing, H.Y. Cui, X.D. Dai, X.M. Liu, Z.F. Yan, Aqueous dye adsorption on ordered mesoporous carbons, J. Colloid Interface Sci. 310 (1) (2007) 83–89.
[23] T.M. Suzuki, M. Mizutani, T. Nakamura, Y. Akimoto, K. Yano, Pore-expansion of organically functionalized monodispersed mesoporous silica spheres and pore-size effects on adsorption and catalytic properties, Microporous Mesoporous Mater. 116 (1–3) (2008) 284–291.
[24] M.H. Sorensen, R.W. Corkery, J.S. Pedersen, J. Rosenholm, P.C. Alberius, Expansion of the F127-templated mesostructure in aerosol-generated particles by using polypropylene glycol as a swelling agent, Microporous Mesoporous Mater. 113 (1–3) (2008) 1–13.
[25] A. Sayari, Y. Yang, M. Kruk, M. Jaroniec, Expanding the pore size of MCM-41 silicas: use of amines as expanders in direct synthesis and postsynthesis procedures, J. Phys. Chem. B 103 (18) (1999) 3651–3658.
[26] A. Tuel, Modification of mesoporous silicas by incorporation of heteroelements in the framework, Microporous Mesoporous Mater. 27 (2–3) (1999) 151–169.
[27] J.L. Blin, B.L. Su, Tailoring pore size of ordered mesoporous silicas using one or two organic auxiliaries as expanders, Langmuir 18 (13) (2002) 5303–5308.
[28] D. Jiang, J. Gao, J. Yang, W. Su, Q. Yang, C. Li, Mesoporous ethane–silicas functionalized with trans-(1R,2R)-diaminocyclohexane: relation between structure and catalytic properties in asymmetric transfer hydrogenation, Microporous Mesoporous Mater. 105 (1–2) (2007) 204–210.
[29] M. Kruk, M. Jaroniec, A. Sayari, New insights into pore-size expansion of mesoporous silicates using long-chain amines, Microporous Mesoporous Mater. 35–36 (2000) 545–553.
[30] A.R. Cestari, E.F.S. Vieira, G.S. Vieira, L.P. Costa, A.M.G. Tavares, W. Loh, C. Airoldi, The removal of reactive dyes from aqueous solutions using chemically modified mesoporous silica in the presence of anionic surfactant—the temperature dependence and a thermodynamic multivariate analysis, J. Hazard. Mater. 161 (1) (2009) 307–316.
[31] D. Lin-Vien, N.B. Colthup, W.G. Fately, J.G. Grasselli, The Handbook of Infrared and Raman Characteristic Frequencies of Organic Molecules, Academic Press, London, 1991.
[32] K.F. Lam, K.Y. Ho, K.L. Yeung, G. McKay, Selective adsorbents from chemically modified ordered mesoporous silica, Stud. Surf. Sci. Catal. 154 (3) (2004) 2981–2986.
[33] L.D. White, C.P. Tripp, Reaction of (3-aminopropyl)dimethylethoxysilane with amine catalysts on silica surfaces, J. Colloid Interface Sci. 232 (2) (2000) 400–407.
[34] K.Y. Ho, G. McKay, K.L. Yeung, Selective adsorbents from ordered mesoporous silica, Langmuir 19 (7) (2003) 3019–3024.
[35] G. Calleja, R.V. Grieken, R. Garcia, J.A. Melero, J. Zglesias, Preparation of titanium molecular species supported on mesostructured silica by different grafting methods, J. Mol. Catal. A: Chem. 182–183 (2002) 215–225.
[36] M. Kruk, M. Jaroniec, A. Sayari, A unified interpretation of high-temperature pore size expansion processes in MCM-41 mesoporous silicas, J. Phys. Chem. B 103 (22) (1999) 4590–4598.
[37] J.F. Yao, H.T. Wang, K.Y. Chan, L.X. Zhang, N.P. Xu, Incorporating organic polymer into silica walls: a novel strategy for synthesis of templated mesoporous silica with tunable pore structure, Microporous Mesoporous Mater. 82 (1–2) (2005) 183–189.
[38] X.B. Liu, F.X. Chang, L. Xu, Y. Yang, P. Tian, L.H. Qu, Z.M. Liu, Preparation of ordered carbon/silica hybrid mesoporous materials with specific pore size expansion, Microporous Mesoporous Mater. 79 (1–3) (2005) 269–273.
[39] H. Dhaouadi, F.M. Henni, Textile mill effluent decolorization using crude dehydrated sewage sludge, Chem. Eng. J. 138 (2008) 111–119.
[40] S. Chatterjee, S. Chatterjee, B.P. Chatterjee, A.R. Das, A.K. Guha, Adsorption of a model anionic dye, eosin Y, from aqueous solution by chitosan hydrobeads, J. Colloid Interface Sci. 288 (1) (2005) 30–35.
[41] A. Vinu, K.Z. Hossain, G. Satish Kumar, K. Ariga, Adsorption of L-histidine over mesoporous carbon molecular sieves, Carbon 44 (3) (2006) 530–536.
[42] S. Akgol, Y. Yalcinkaya, G. Bayramoglu, A. Denizli, M.Y. Arica, Reversible immobilization of urease onto Procion Brown MX-5BR-Ni(II) attached polyamide hollow-fibre membranes, Process Biochem. 38 (5) (2002) 675–683.
[43] I. Langmuir, The constitution and fundamental properties of solids and liquids, J. Am. Chem. Soc. 38 (11) (1916) 2221–2295.
[44] I. Langmuir, The adsorption of gases on plane surfaces of glass, mica and platinum, J. Am. Chem. Soc. 40 (9) (1918) 1361–1403.
[45] B.C. Pan, Y. Xiong, A.M. Li, J.L. Chen, Q.X. Zhang, X.Y. Jin, Adsorption of aromatic acids on an aminated hypercrosslinked macroporous polymer, React. Funct. Polym. 53 (2–3) (2002) 63–72.
[46] Z. Reddad, C. Gerente, Y. Andres, P.L. Cloirec, Adsorption of several metal ions onto a low-cost biosorbent: kinetic and equilibrium studies, Environ. Sci. Technol. 36 (9) (2002) 2067–2073.
[47] O. Redlich, D.L. Peterson, A useful adsorption isotherm, J. Phys. Chem. 63 (6) (1959) 1024.
[48] S.K. Das, J. Bhowal, A.R. Das, A.K. Guha, Adsorption behavior of rhodamine B on *Rhizopus oryzae* biomass, Langmuir 22 (17) (2006) 7265–7272.
[49] S. Wang, Y. Boyjoo, A. Choueib, Z.H. Zhu, Removal of dyes from aqueous solution using fly ash and red mud, Water Res. 39 (1) (2005) 129–138.
[50] I.D. Mall, V.C. Srivastava, G.V.A. Kumar, I.M. Mishra, Characterization and utilization of mesoporous fertilizer plant waste carbon for adsorptive removal of dyes from aqueous solution, Colloids Surf. A: Physicochem. Eng. Aspects 278 (1–3) (2006) 175–187.

[51] K.V. Kumar, Linear and non-linear regression analysis for the adsorption kinetics of methylene blue onto activated carbon, J. Hazard. Mater. 137 (3) (2006) 1538–1544.
[52] D. Ghosh, K. Bhattacharyya, Adsorption of methylene blue on kaolinite, Appl. Clay Sci. 20 (6) (2002) 295–300.
[53] M.S. Chiou, P.Y. Ho, H.Y. Li, Adsorption of anionic dyes in acid solutions using chemically cross-linked chitosan beads, Dyes Pigments 60 (1) (2004) 69–84.
[54] D.D. Asouhidou, K.S. Triantafyllidis, N.K. Lazaridis, K.A. Matis, S.S. Kim, T.J. Pinnavaia, Sorption of reactive dyes from aqueous solutions by ordered hexagonal and disordered mesoporous carbons, Microporous Mesoporous Mater. 117 (1–2) (2009) 257–267.